Project Number: DJO-0510

Re-Design of a Thermal Energy Scavenging System for a Gas Turbine

A Major Qualifying Project Report:

Submitted to the Faculty of

WORCESTER POLYTECHINC INSTITUTE

in partial fulfillment of the requirements for the

Degree of Bachelor of Science

by

Joseph Miller, Austin Ng, Kile Simpson, Jonathan Sullivan

4/5/2010

Advisor: David Olinger

Co-advisor: Simon Evans

Abstract

The goal of this project was to develop a thermoelectric scavenging device for use on a Pratt and Whitney gas turbine engine during static testing. Design requirements include an overall system size of less than 3”x3”x3” and the ability to produce a steady 10V at 300 mA. This project extended previous efforts by a WPI MQP group. Modifications were made to many of the original components to further the goal of creating a more robust assembly. Computer models were created and examined in parallel with experimental results to select optimized configurations and operating conditions. Vibration and thermal failure modes were analyzed to ensure the final design would function in the test environment. Finally, an endurance test was run on a hot steam pipe in the WPI Powerhouse to simulate use by a client in the field. The device successfully converts thermal energy into electricity but at a lower power levels than required by Pratt and Whitney. Suggested solutions are provided to overcome the lack of adequate power generation.

Contents

List of Figures

List of Tables

1 Introduction

In the process of jet engine testing and validation, one of the major costs is the set up of the thousands of sensors that are required to fully observe how the engine performs. Mainly sensors collect pressure and temperature data in order to calculate engine characteristics such as specific fuel consumption, static and stagnation pressure ratios, and temperature ratios. As seen in Figure 1-2, an engine setup can be quite complex. It can take thousands of man hours to prepare a test, which translates into tens of thousands of dollars.

Figure 1-1: Engine During Testing (Def10)

Each set of sensors requires two sets of cabling, namely power and data transfer lines. The data transfer lines can be fairly easily eliminated with a wireless data transmitter. Unless the need for an external power supply can be eliminated, the savings would be marginal. The purpose of this project is to design, build, and test an energy scavenging system that can be implemented in order to fill this demand.

2 Design Requirements

Each energy scavenging system must measure less than 3”x3”x3”, produce roughly 10V at 0.3 A, and be able to withstand a temperature of up to 2000°F. The unit must continuously provide stable power before engine start up, throughout the testing, and after engine shutdown. It must also be able to withstand the harsh environment that it will operate in without need of repair. It must also be affordable, and practical in order to be implemented on a full scale at Pratt and Whitney. The precise requirements and constraints are listed in bullet form below, for ease of reference.

2.1 Requirements

- 10 V at 0.3 A
- Continuous power delivery before “firing” of engine
- Continuous operations for 100+ hours
- Withstand temperatures of up to 2000 F
- Maintenance free

2.2 Design Constraints

- 3”x3”x3” Volume
- No chance of engine damage
- Fairly inexpensive

3 Previous Work

This project is a continuation of an MQP project by Bradway et al (2008). The initial project had the goals of building a proof of concept device that would harvest excess energy from an active jet engine to power test sensors. Many feet of wiring along with hundreds of hours used in setup time would be able to be saved by using a device to scavenge this excess energy and so Pratt and Whitney, an Aerospace and Defense company, took the role of sponsor for the project.

Bradway et al (2008) identified available sources of energy scavenging from turbine engines to be thermal, vibrational and piezoelectric. By examining past research they were able to determine that both vibrational and piezoelectric methods, for the 3”x3”x3” volume limit required, could not generate the desired power. Thermal energy scavenging was found to be the most viable solution due to both the abundance of research in the field and the relative ease of use. Many manufacturers offer Thermo-Electric Generators (TEGs) and basic heat transfer theory is very accessible making thermal energy scavenging a very practical solution.

When designing the assembly, Bradway et al (2008) had a number of design decisions to make. First, they had to select an appropriate TEG to maximize power while minimizing cost and size. They selected a TEG from the supplier Tellurex that was approximately 2.1”x2.1” in cross section and 0.125” thick. Because of these dimensions, only one TEG could be used in the desired 3”x3” cross section. To maximize the possible output of this generator, the ΔT had to be maximized across it. This was done with a heat sink attachment, and later with a table fan forcing air over the heat sink. In order to maximize the transfer of heat to and from the

generator, aluminum plates were fabricated to envelop it.

One of the Pratt and Whitney's requirements of the generator assembly was that the device would operate during start-up of the engine, even before excess heat was generated. To solve this problem, a rechargeable battery pack was introduced into the design. Bradway et al (2008) chose Lithium Ion batteries because of their longevity. A dual-power electric circuit was then designed to draw power from the batteries during transient and low temperature periods, and to charge the batteries when excess energy was available. The circuit was designed and tested successfully.

During testing, desirable voltages and currents were achieved through the use of a large external fan. The batteries and most electronics were left off of the hot plate used for testing to prevent thermal failure, and they acknowledge the large table fan used will be unfeasible for a production model, but their results certify the proof of concept that this device can meet the power requirements of Pratt and Whitney.

4 Background Theory

4.1 The Seebeck Principle

The thermo electric generators, as stated above, work through the Seebeck principle. In 1821, Thomas Seebeck discovered the thermocouple when he noted that two electrically conductive metals are separated along their length but connected at their ends and exposed to different temperatures, a magnetic field is generated at the legs (Encyclopedia Britannica, 2010). The ratio of temperature difference across the metals to the voltage generated by the magnetic field is called the Seebeck coefficient. These thermocouples can be wired in series to create an array called a thermopile which is placed between ceramic plates to withstand high temperatures (TEG Power, 2009).

4.2 Heat Sinks

As will be discussed in §5.1, a heat sink was used to increase heat dissipation from the generator. This decision was made similarly to that of Bradway et al (2008). Heat sinks utilize fins protruding from their surface to increase their total surface area. This increased surface area allows for much higher rates of cooling than would be possible with the generator exposed to ambient air. By increasing this cooling, the effectiveness of the Seebeck principle can likewise be increased. The goal is to maximize the hot side temperature and minimize the cool side without using active cooling such as fans. This allows all energy harvested to be used by the load and keeps the volume of the assembly within the allowable envelope.

5 Design Alternatives

5.1 Assembly

The direction taken in the design process was straightforward from the description of the project and the limiting dimensions and factors. The original design for this project consisted of, from bottom to top; an aluminum base plate, the thermoelectric generators, a heat sink, a fan, and electronics boxes. There was to be an insert milled into the heat sink to allow for flush contact between the generators and the sink.

The first design revision can be seen in Figure 5-1. The black ribbon seen in Figure 5-1 is a silicone insert designed to insulate the heat sink from the aluminum plate. The silicone gasket will force the heat flow to go through the generators, allowing the device to reach maximum effectiveness.

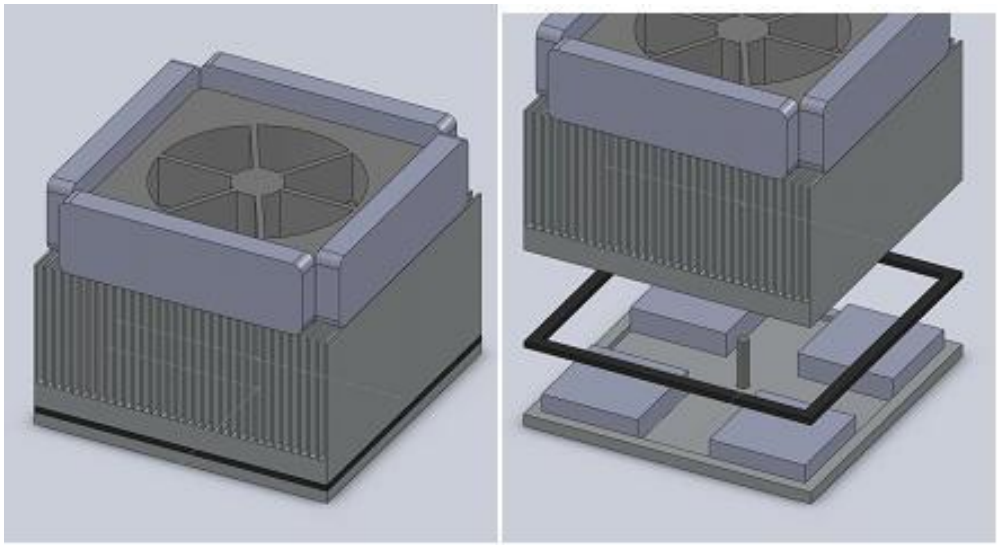

Figure 5-1 Original Assembly

As a result of budgetary constraints the four generator design was not a viable option, therefore the design was altered to fit two generators instead. The change from four generators to two will be shown in the decreased performance of the device. The decrease will be linear and will be accounted for in the results section. The results from initial testing showed that the fans were not significantly increasing performance and were removed from the design to fully utilize the power generated by the device. The final assembly is shown in Figure 5-2. The final design allows for the electronics to be placed on the side of the heat sink. Two screws were added instead of one so that the bottom plate and heat sink could not rotate.

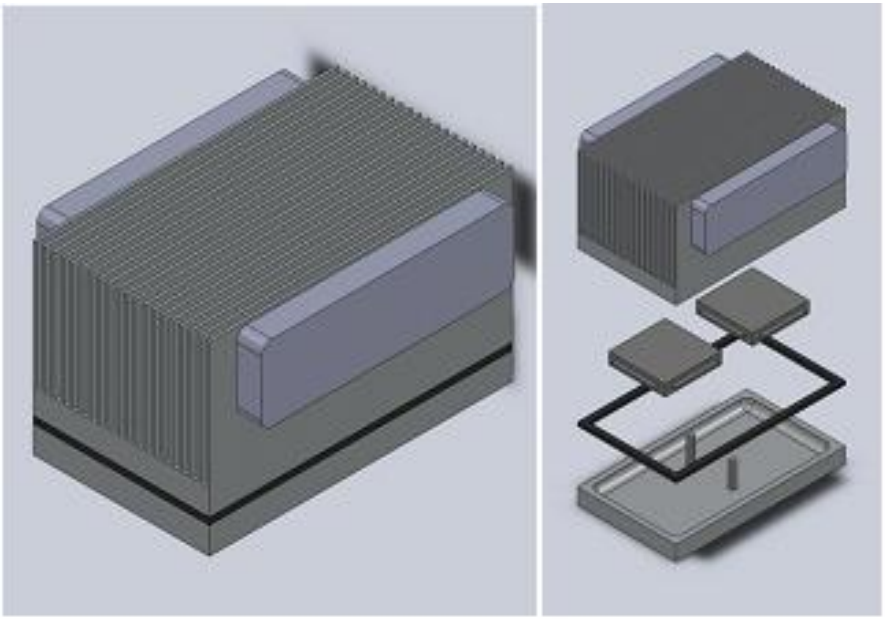

Figure 5-2 Second Generation Assembly

Because the base plate of the heat sink was so thin, the milled insert was moved to the heat sink. This feature allows for more flexibility in the design by creating a quick change interface between heat sinks.. To test new heat sinks using the original design each sink would have to be precisely machined. In the current design, the only work that needs to be done on a

new heat sink is the tapping of two holes to accommodate the screws that hold the assembly together.

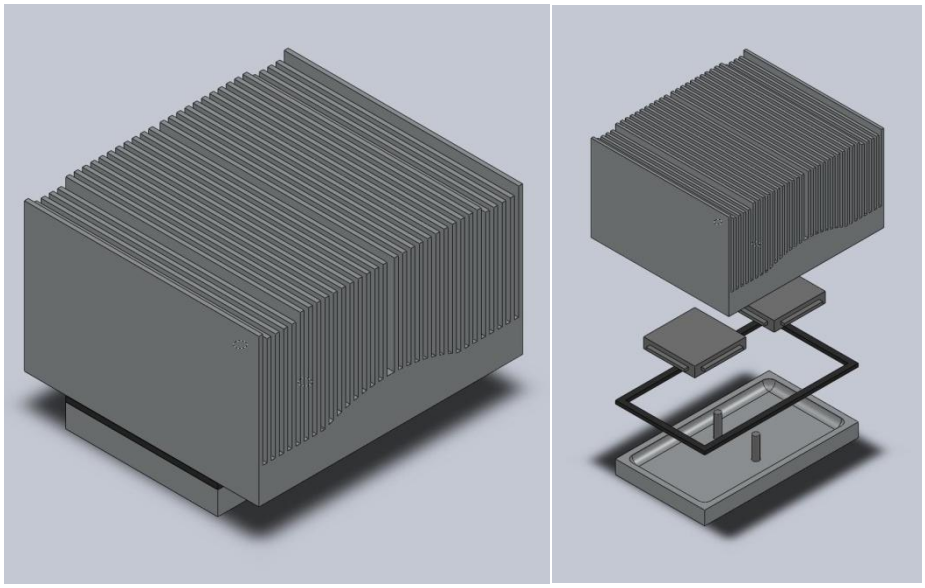

Figure 5-3 Final Assembly as Tested

The final assembly, shown in Figure 4, allows for the electronics to be placed on the side of the heat sink. The configuration of these electronics will be determined by the method that the customer will use to make the circuits discussed in the Circuitry section. During construction the decision was made to use the current heat sink which is larger than shown but still fits within the required dimensions.

The final assembly is easily adjusted to accommodate any number of generators based on the data collected from testing. The only changes would be to the base plate, gasket and heat sink, the rest of the design would stay the same. The finished product's overall structure would not differ except in heat sink dimensions. The performance would be altered based on the heat sink's capabilities.

5.2 Thermal Generators

Table 5-1 Properties of the HZ-2 Module (Hi-Z)

Initially there were two possibilities for thermoelectric generators that appeared to meet the requirements; Hi-Z and TEG Power. TEG Power is a West Virginia based company who created enhanced Seebeck TE modules. The TEG Power Enhanced Seebeck TE Module is capable of creating 5 volts, 1.8 amps, and 9 watts with a temperature gradient of 200C. Hi-Z Technology, Inc. was identified as possessing a product that performed in the range of the TEG Power module but was more expensive.

Properties of the 2 Watt Module, HZ-2		
Physical Properties	Value	Tolerance
Width & Length	1.15" (2.90 cm)	±0.01 (0.25)
Thickness	0.2" (0.508)	±0.01 (0.25)
(Special Order)		±0.002 (0.05)
Weight	13.5 grams	±2 grams
Compressive Yield Stress	3 ksi (20 MPa)	minimum
Number of active couples	97 couples	----
Thermal Properties		
Design Hot Side Temperature	230°C (450°F)	±10 (20)
Design Cold Side Temperature	30°C (85°F)	±5 (10)
Maximum Continuous Temperature	250°C (480°F)	----
Maximum Intermittent Temperature	400°C (750°F)	----
Thermal Conductivity*	0.024 W/cm*K	0.001
Heat Flux*	9.54 W/sqcm	±0.5
Electrical Properties (as a generator)*		
Power**	2.5 Watts	minimum
Load Voltage	3.3 Volts	±0.1
Internal Resistance	4.0 A	±0.05
Current	0.8 Amps	±1
Open Circuit Voltage	6.53 Volts	±0.3
Efficiency	4.50%	minimum

The product is known as the HZ-2 and is 1.15 inches square and .2 inches thick. The HZ-2 module is capable of creating 2.5 Watts and 3.3 Volts at matched loads with a hot side temperature of 230C and a differential of 200C. The HZ-2 is also quite durable with a maximum continuous temperature of 250C and a maximum intermittent temperature of 400C.

The specifications for the HZ-2 are listed in Table 5-1 and, when compared to the specifications for the TEG Power Enhanced Seebeck Module, show that there is very little difference in the two devices and the final unit performance should not suffer.(Hi-Z)

After placing an order with TEG Power they had numerous issues in being able to deliver the final product. The decision was then made to use the HZ-2 as a replacement for the TEG Power generators. As discussed earlier, the dimensions and properties are more than adequate to act as a drop in replacement for the TEG Power enhanced Seebeck modules used in the preliminary design. At the writing of this report TEG Power was no longer producing the Enhanced Seebeck Module.

The HZ-2 and TEG Power modules both work by implementing the Seebeck effect. Seebeck modules are more durable and efficient at converting a temperature differential into usable electricity than the more common Peltier modules. The majority of thermoelectric devices utilize the Peltier effect which is not as robust as the Seebeck module produced by Hi-Z and TEG Power which have a 100F higher temperature threshold. The Seebeck module is also capable of creating 9 watts of power compared to the two watt limit on all 127 thermocouple Peltier modules. The modules are also capable of being connected in parallel or series to increase any desired output from the thermal energy scavenging device.(TEG Power, 2009)

5.3 Batteries

The batteries to be used need to fit several requirements. The batteries must have enough capacity to power the load until the thermoelectric generators begin producing sufficient power. Low self discharge rates are needed to ensure there is power to run the device after idling for long periods of time, as much as three months or more. The batteries should also have the ability to go through many charge cycles without ill effects on the batteries' characteristics.

Many batteries can be eliminated due to the baseline requirements. Rechargeable lithium-coin type batteries, such as those typically used in watches, lacked the capacity needed in this application. Standard Ni-Cd rechargeable and Ni-MH have poor self-discharge characteristics, losing as much as 30% of their capacity per month at room temperature, with self discharge rates increasing with increasing temperatures. Rechargeable alkaline batteries have poor cycle life. Lithium-ion batteries will permanently lose capacity if constantly charged for periods of time, and have more catastrophic failure modes with the possibility of exploding if overcharged or overheated.

Low self discharge Ni-MH batteries were found to be a good match for this application. Low self discharge Ni-MH rechargeable batteries have lower self discharge rates because of three changes from the traditional Ni-MH battery. A different material for the negative electrode is used, additional additives are used in the positive electrode, and using a different separator between the electrodes. These all result in a lower self-discharge rate, with the batteries only losing 5% to 10% of their capacity per month. From the graphs provided by Sanyo, after three months of sitting idle, the batteries retain over 90% of their capacity as

shown in Figure 5-5. Even at the reduced capacity, it is expected that the batteries will provide enough power to allow the sensors to be run during the time the thermoelectric generators will need to reach operating temperatures. The batteries are also rated to be recharged over 1000 times before significant degradation in storage capacity occurs, as seen in Figure 5-4. This will allow the device to be run without the need to replace batteries after many test cycles. From the material safety datasheet (SANYO), the maximum temperature before the batteries begin to fail is 212°F at which point they may begin to leak electrolyte, which can cause skin burns if handled without proper safety gear. Should the batteries fail from high temperature, this is relatively mild and manageable and should not damage any other components of the device

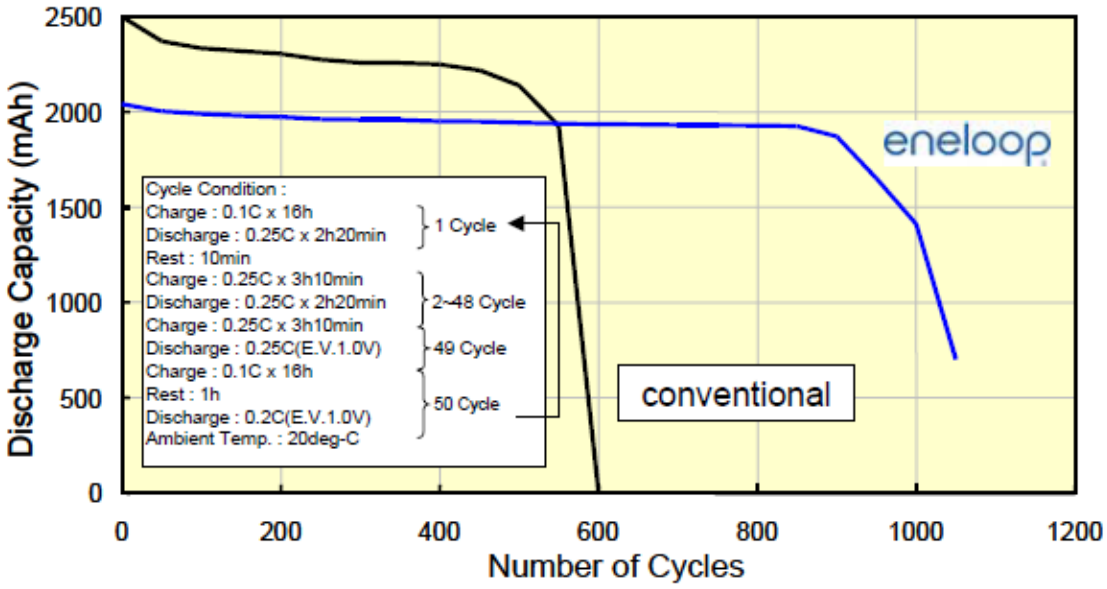

Figure 5-4 Discharge Capacity of Ni-MH Batteries (Teraoka)

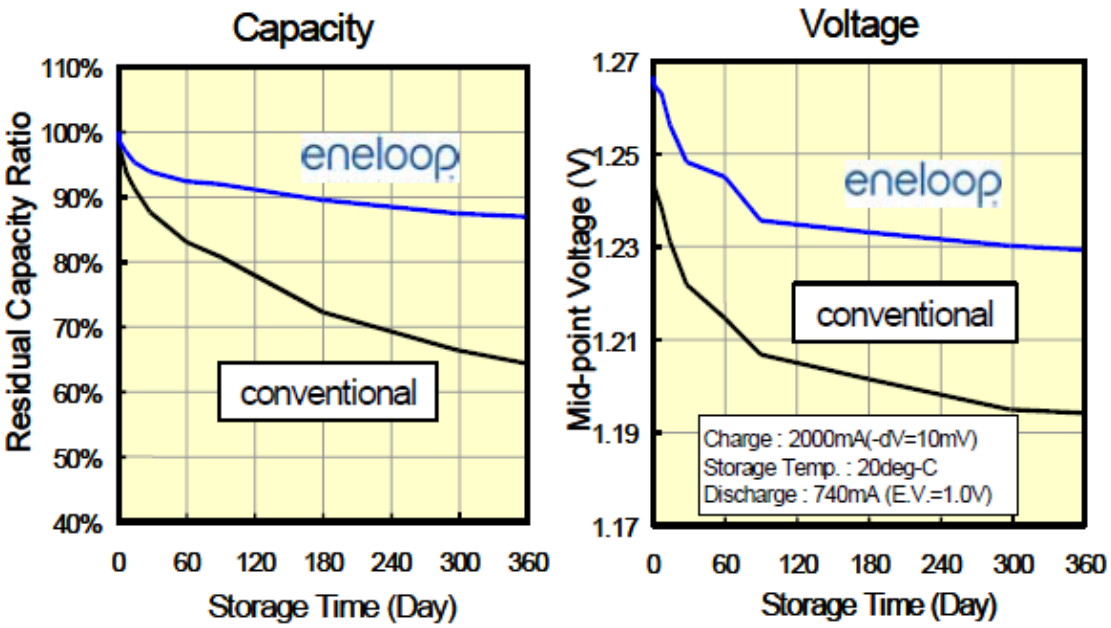

Figure 5-5 Storage Time Performance of Ni-MH Batteries (Teraoka)

5.4 Circuitry

One major design task is routing the desired energy from the thermoelectric generators into the array of sensors and data transmitters. Under normal circumstances, the idea of transporting electrical energy might not seem to be much of a challenge, but this is not an ordinary application. Temperatures immediately surrounding the thermoelectric generator can be as high as 250 °C, much hotter than most electronics can operate. Also, because of temperature variations with time, the energy produced is not constant. These sensors require a constant energy supply. Finally, the batteries will need to be on a smart circuit to either charge or drain them during the test.

The first challenge is to remain well within the operating temperature of each of the components in the circuitry. As discussed earlier, the batteries have max temperature of 50 °C. Standard electronic components operate at a ceiling of roughly 50 °C. It is paramount that the temperature of the electronics does not exceed their capabilities. Active cooling has the potential to increase the voltage generated at a cost of using generated power. This may result in less net power generated than passive cooling. This will be discussed in further detail later on.

Ideally, the energy created by the thermoelectric generator is constant and steady. This assumes that all temperatures, cooling rates and energy dissipation are constant at steady state. In a real life situation, this scenario is extremely unlikely. A means must be provided in order to account for such perturbations in the nominal conditions.

In order to ensure a constant energy distribution, either the temperatures must remain constant at their nominal conditions, or a circuit must be designed in which the voltage is regulated at a given quantity. To be able to keep the temperatures nominal would require a degree of sophistication, complexity, and cost that is not in the scope of this project. Fortunately it is much easier, simpler, and cost effective to create what is known as a voltage stabilizer.

A voltage stabilizer is a relatively simple circuit that uses a shunt regulator in order to maintain a constant voltage. A shunt regulator, such as a Zener diode, will begin conducting at a specified voltage. The shunt regulator will conduct as much current as required to hold its terminal voltage in order to maintain the desired voltage.

A transistor is a rather innovative electronic component which has revolutionized electronics since its introduction in 1960. It has a variety of uses which include, but aren't limited to amplification and switching. In this particular application, we are most concerned with the switching application of the transistor. The Zener diode used in series with a transistor will stabilize any voltage produced by the thermoelectric generators, assuming that Vin is 0.7 V greater than the design voltage Vout.

In order to validate the theory, the previous circuit as pictured in Figure 5-10 needs to be analyzed computationally with software. Although more sophisticated and complex analysis tools exist, for our purposes and budget, PSICE will be sufficient. As specified by Pratt & Whitney, the sensors will draw 0.3 A at 10 V. Using Ohms Law, Equation 1, the equivalent resistance can be calculated as 33.3 Ohms.

$$\frac{V}{I} = R \quad (1)$$

The above calculated equivalent resistance will be used for R2 in the simulation in order to model the circuit. The Zener Diode, D1, is chosen to be a 1N740A 10V 1W diode. This should supply 10 V to the collector of the transistor and thus supply ~ 10V to the load. In this model, the thermo electric generators are simulated by a DC and AC voltage supply, placed in series, creating a sinusoidal Vin that is modeled by Equation 2. This will simulate a varying voltage ranging from 12.75 to 13.25 V with a period of 1 second.

$$V_{in} = 13 + 0.25 * \sin(\frac{t}{2 * \pi}) \quad (2)$$

Figure 5-6 displays the input and output of the voltage stabilizer as a function of time. This input is shown by the red line labeled V(V2:+) and the output is shown by the blue line labeled V(R2:2). As can be shown, the amplitude of voltage oscillation is reduced by a factor of 2.

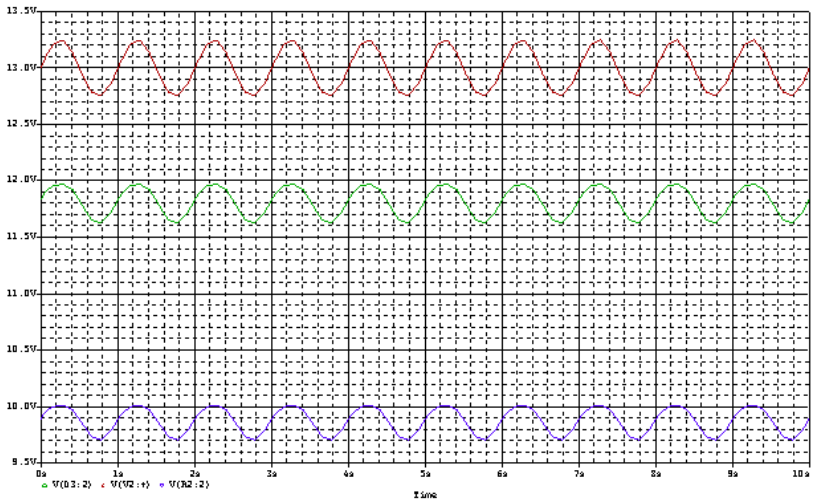

Figure 5-6 Voltage Stabilizer

The dampening is even more dramatic if the nominal input voltage is raised to 14.75V as shown in Figure 5-7.

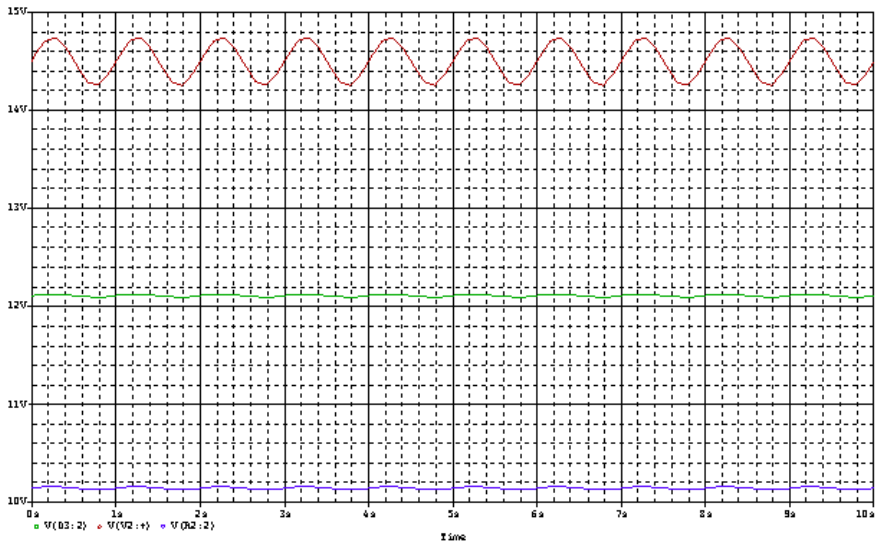

Figure 5-7 14.75 Volt Circuit

Unfortunately, this presents another problem. In order to produce a stable 10.2V output, we need to generate at least 14.75V from the thermo electric generator. One TEG only produces, at most, 2.45 V at a hot side temperature of 200 °C and cool side of 50 °C. A DC to DC converter can be used in order to step up the voltage to the required value, while conserving power. The output of the integrated circuit is governed by the following equation, Equation 3. The power in $\boldsymbol{V_{in} * I_{in}}$ must equal the power out $\boldsymbol{V_{out} * I_{out}}$ divided by the efficiency of the integrated circuit.

$$\boldsymbol{V_{in} * I_{in} = \frac{V_{out} * I_{out}}{\eta_{ic}}} \quad (3)$$

As stated by Hi-Z specs, at a hot side temperature of 200 °C and a cool side of 50 °C, each module produces a maximum power of 1.86 W at matched loads (Hi-Z). As stated by Pratt & Whitney, 10V at 0.3A of electricity is required. This equates to 3 W of electricity. Therefore, using Equation 3, an efficiency of 80.6% is required for the system.

A MAX863 is used in order to step up the voltage to the needed 10V. Key parameters of the IC are shown in the following chart, Figure 5-8. Figure 5-9 shows how to use the MAX863 in a circuit.

	MAX863
Efficiency	90%
Vout Max	24 V
I @ Vout of 10V	337 mA
Vin Min	1.7 V
Operating Temp	-40°C to +85°C

Figure 5-8 MAX863 Performance Table

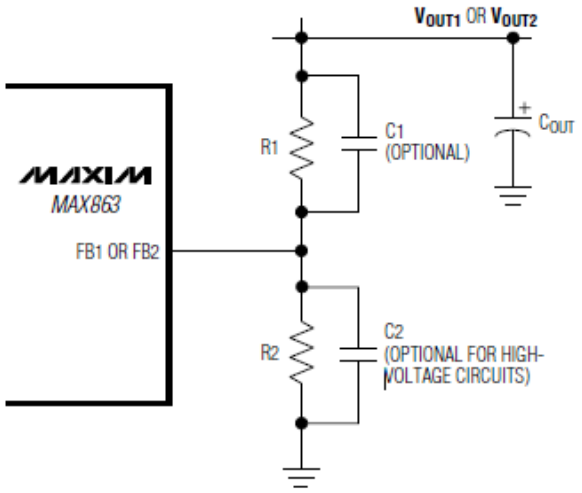

Figure 5-9 Voltage Selector

In order to select the output voltage required, the following formula can be used, where R1 and R2 are as labeled in Figure 5-9. R2 is recommended to be in the 10kΩ to 500kΩ range. Stepping through Equation 4, the ratio R1/R2 can be found to be 7.

$$\boldsymbol{R1 = R2 * \left(\frac{Vout}{1.25} - 1\right)} \tag{4}$$

The external circuit required to support a step up to 10V is shown below in Figure 5-10. All components are readily available and pose no problems for manufacturing a printed circuit board.

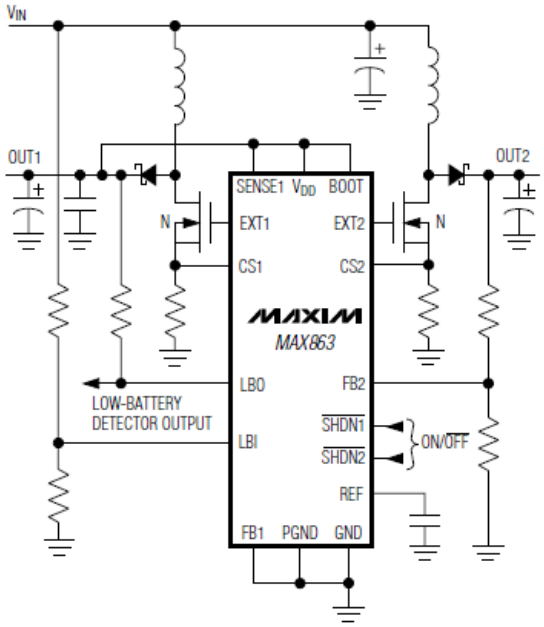

Figure 5-10 Voltage Stabilizing Circuit

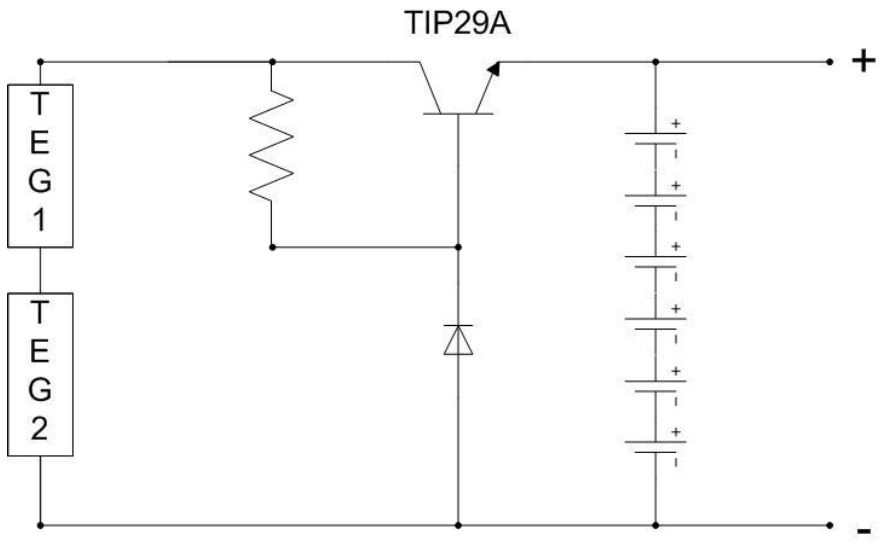

Figure 5-11 Voltage Stabilization Circuit

Battery power must be utilized during engine startup times when little to no thermal energy will be produced. To avoid the hassle of changing the batteries, rechargeable NiMH batteries have been chosen as discussed in §5.3. Charging can be done by putting the batteries in parallel with the load resistance. The net voltage across the batteries is defined by the following equation, Equation 5:

$$\boldsymbol{V_{net} = V_{generated} - V_{batteries}} \quad \textbf{(5)}$$

During startup, the generated voltage is equal to 0 and the battery voltage, assuming they are fully charged, is equal to -9 V. The resulting net voltage is -9V. As the batteries drain and the transient stage is passed, the thermoelectric generators will produce a stabilized voltage. Now the generated voltage will be 9 V and the voltage of the batteries (which have been slightly drained) will be lower, i.e. 8.8 V. According to Equation 5, the resulting net voltage across the batteries will be equal to +0.2 V. The batteries will trickle charge at 0.2 V. With each

battery having an internal resistance of 40 mΩ, the resulting current produced would be 833 mA; a value typical among NiMH battery chargers. This system of charging is inherently stable. As soon as the batteries reach full capacity, 9 V, the voltage differential is reduced to 0, preventing overcharging which can ruin the battery life.

5.5 Materials

Heat transfer performance can, in certain situations, be drastically improved using alternative materials. Aluminum plates and an aluminum heat sink were used in previous testing and were marked as baseline performance for the assembly. An examination was done to discover if alternate materials would improve the performance of the device.

The heat sink was chosen experimentally by Bradway et al (2008) comparing the results of a pinned copper heat sink against two different finned aluminum heat sinks. Despite having different fin configurations, the difference in performance was significant enough that Bradway et al (2008) were confident in selecting aluminum as the dominant material.

The material of the plates housing the TEG was also examined. These plates facilitate the heat transfer both to and from the generator, so high thermal conductivities were desired. Insulating materials such as ceramics would prevent heat from reaching the generator's hot side and also negatively impact dissipation of heat from the cool side. The bubble plot shown in Figure 5-12 was created using the CES Edupack Granta (Granta Design Limited, 2009) package comparing the thermal conductivity (k) of many metals and ceramics. Because the budget for the project is limited, these k values were plotted against price/mass of the material.

As can be seen in Figure 5-12, for the same price range only copper has a higher k than aluminum. To see the effect of increasing the thermal conductivity of the plates, a short Matlab script was written utilizing the thermal resistance method explained in §6.1 . The script plots the expected 'cool side' temperature of the TEG exposed to ambient air, with no heat sink, against the thermal conductivity of the sandwiching plates. Equation 6 was used to generate the results plotted in Figure 5-13. The code can be found in Appendix B, Material

Selection Code.

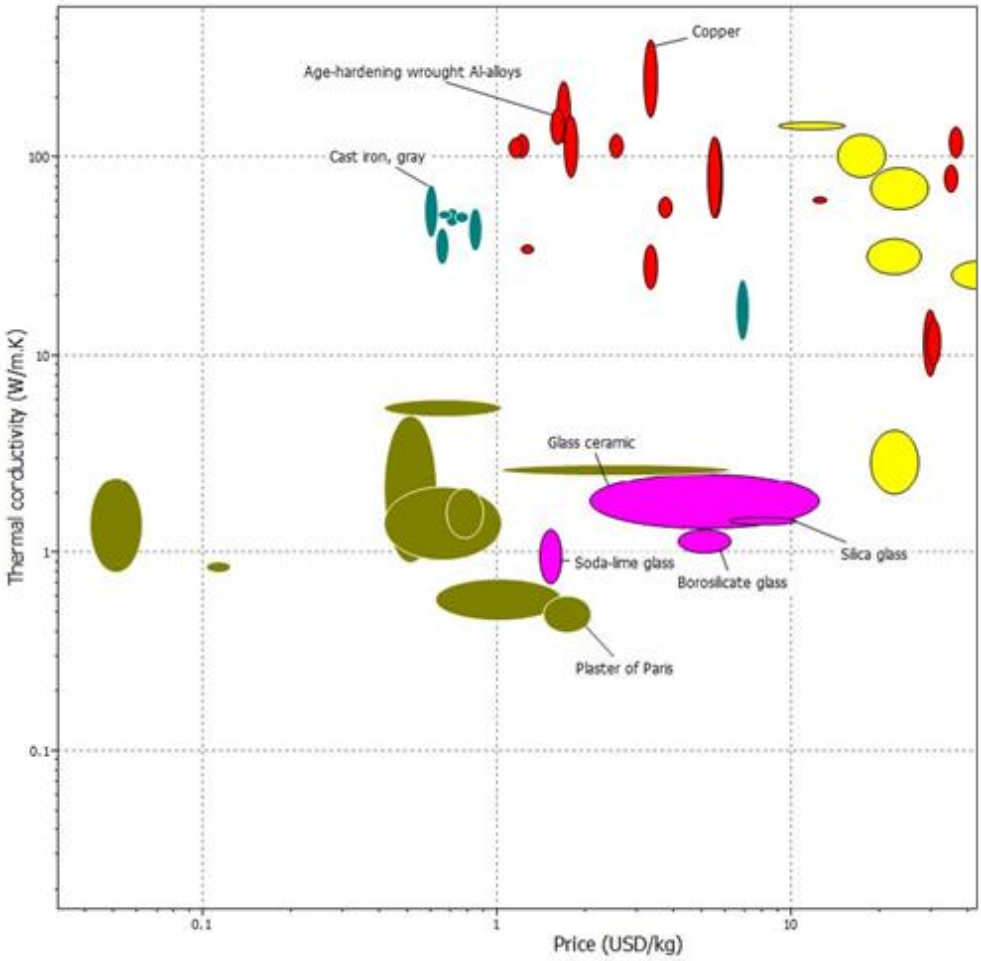

Figure 5-12 Thermal Conductivity against Price for common materials

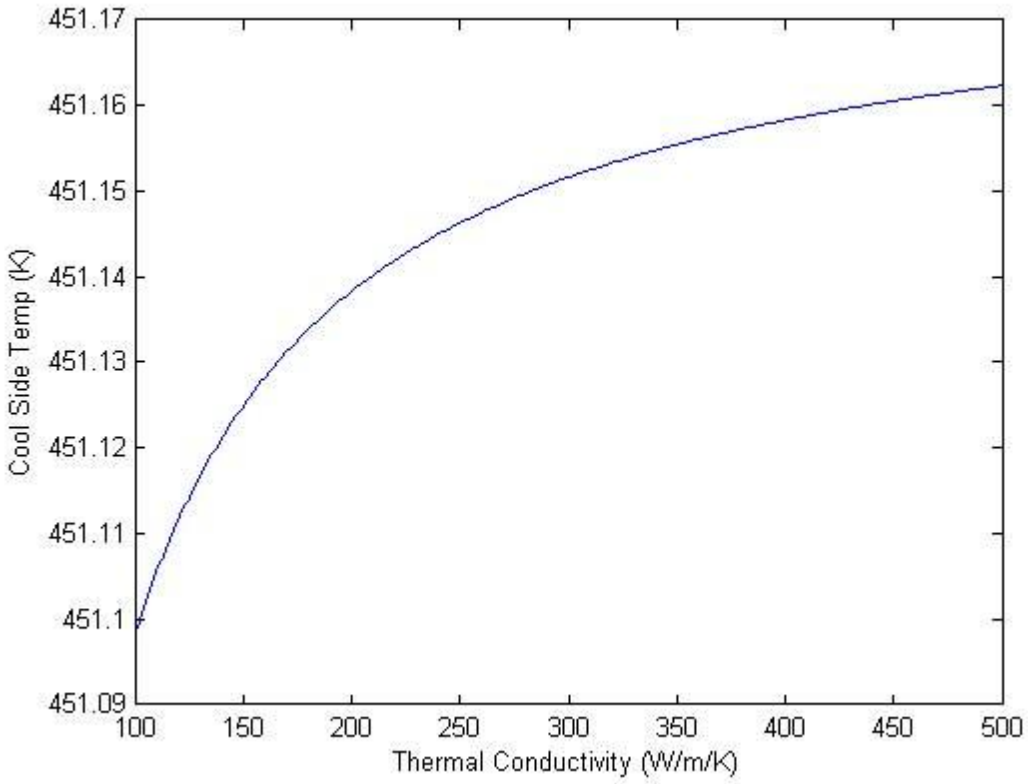

Figure 5-13 Thermal Conductivity against Temperature Drop for common materials

$$T_{Cool} = T_{Hot} - \frac{(T_{Hot} - T_{\infty})}{\left(2\frac{t_{Mat}}{k_{Mat}} + \frac{t_{Gen}}{k_{Gen}} + \frac{t_{Air}}{k_{Air}}\right)} \cdot \left(2\frac{t_{Mat}}{k_{Mat}} + \frac{t_{Gen}}{k_{Gen}}\right) \quad (6)$$

The cool side temperature in the model varies by only 0.07 K over a conductivity range of 400 W/m-K. This is insignificant and, as such, aluminum will remain the material of choice for cost and ease of acquisition reasons.

5.6 The Final Design

The final design used in testing was a two HZ-2 TEG design with an oversized heat sink. Using two TEGs removed budget as a constraint but still allowed for relevant testing to be done. The final circuit could not be fabricated due to issues with the IC; a micro IC was delivered that was incompatible with the breadboards available. High temperature wiring was used to extend the leads of the TEGs to the circuitry.

The final design, shown in Figure 5-14, allowed for the electronics to be placed on the side of the heat sink. The heat sink remained cool enough to prevent damage to electronics, and the addition of dual sided, thermally insulating tape to secure the electronics further increased the margin of safety.

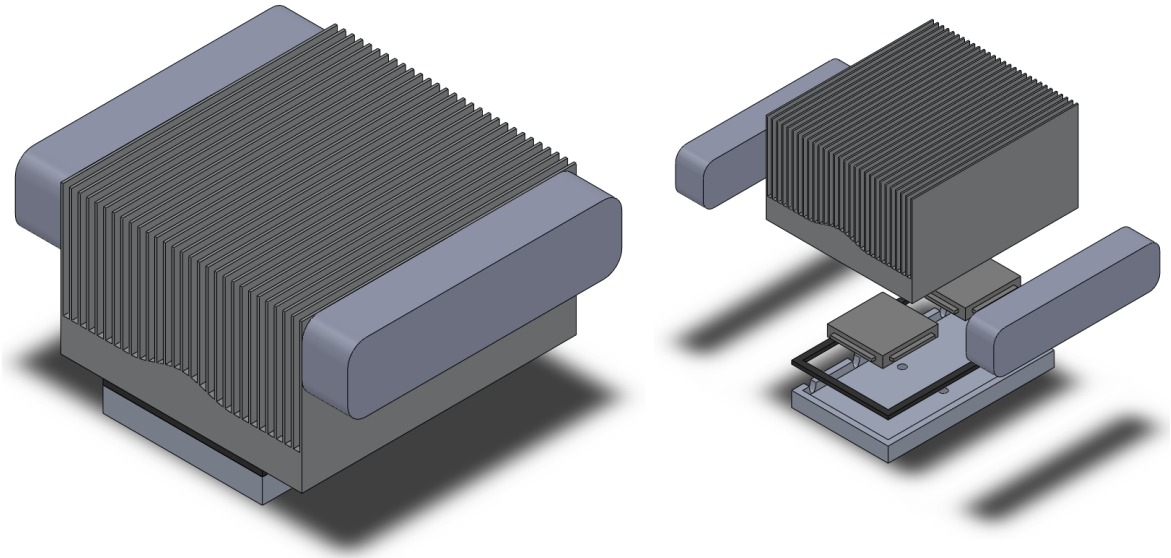

Figure 5-14 The Final Assembly Design

6 Simulations

6.1 Matlab Simulation

Throughout the design of the thermoelectric generator, many questions were raised about performance should one aspect or another be adjusted. Rather than build many different iterations of the assembly to test the performance of each under different configurations, the obvious conclusion was drawn that a computerized model would be ideal. Matlab was used to write the main simulation and results were compared to SolidWorks models in addition to the actual performance of the assembly. Matlab was used because of its ubiquity in engineering settings, its relative speed in dealing with simple scripts and its lack of overhead due to its powerful built-in graphing capabilities.

The most important topics to be investigated with the model were the performance of different heat sinks and whether or not passive cooling would be powerful enough to achieve the required results. The model was written to output various key temperatures and the expected voltage generation given different initial conditions. The purpose of the model was to create an appreciable correlation between expectations and real performance with a relatively simple model at a reasonable level of accuracy. Limited assumptions were made during the modeling process to further this goal.

After various iterations of solution methods, it was decided to use the thermal resistance of each piece of the assembly to create a thermal circuit. This circuit could then be evaluated as an electric circuit and points of interest easily backed out from the final solutions (Incropera, et al., 2006). Each piece of the assembly has its own resistance measured in °C/W,

the temperature drop across the piece divided by the heat flow through it. These resistances are then assembled according to their position in the assembly and summed as electrical resistors to find a total, effective resistance for the entire thermal circuit. The circuit used for the model is diagrammed in Figure 6-1 below.

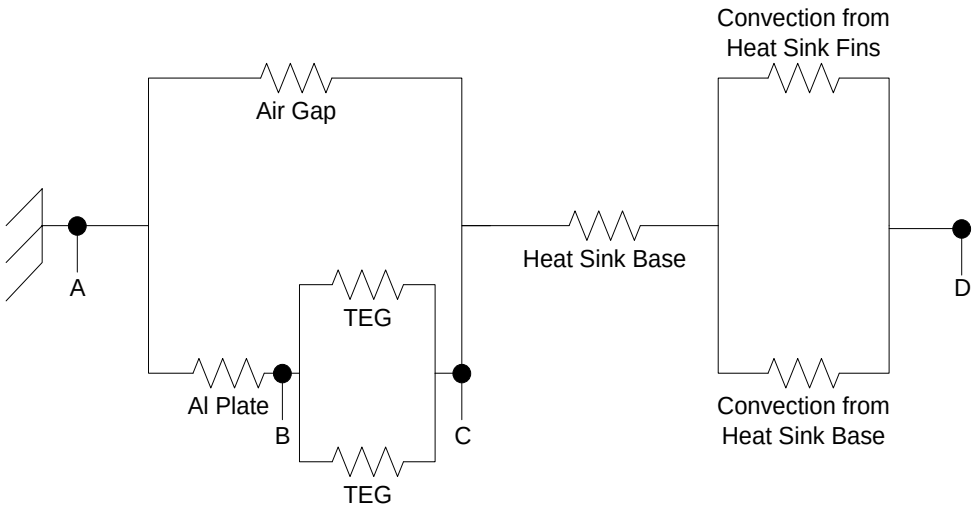

Figure 6-1 Thermal Circuit for Matlab Model

Newton's law of cooling was used to calculate the thermal resistance of each element. Equation 6 and Equation 7 are the equations of heat transfer for conduction and convection, respectively. A in each of the equations is the cross sectional area of the element normal to the direction of heat flow. In Equation 7, L is the thickness of the material in the direction of heat flow. The h in Equation 8 is the convective heat transfer coefficient. This term generally needs to be experimentally determined as it depends so heavily on the properties of the gas (Incropera, et al., 2006).

$$q_{cond} = \frac{kA}{L}\Delta T \tag{7}$$

$$q_{conv} = hA\Delta T \tag{8}$$

The thermal resistance for each element, R_n, can be calculated using Equation 9, where n is the element number.

$$R_n = \frac{\Delta T_n}{q_n} \tag{9}$$

According to the method, the heat flow, q, through each section of the thermal circuit is a constant, i.e.: $q_n = q$. The heat flow, q, is equivalent to the current through an electrical circuit. This constant heat flow can be calculated from the effective resistance of the entire circuit, R_{Tot}. By calculating R_{Tot} and having knowledge of the temperature of the heat source (Point A in Figure 6-1) and the temperature of ambient air (Point D in Figure 6-1), q can be calculated. The total resistance is calculated in Equations 10 and 11 by summing the resistances together as one would in the equivalent electrical circuit.

$$R_{Tot} = \frac{\Delta T_{Tot}}{q} \tag{10}$$

$$R_{Tot} = \left[\frac{1}{\frac{L_{BP}}{k_{BP}A_{BP}} + \frac{L_{TEG}}{2k_{TEG}A_{TEG}}} + \frac{1}{\frac{L_{BP}+L_{TEG}}{k_{Air}(A_{HSBP}-A_{BP})}}\right]^{-1} + \frac{L_{HSBP}}{k_{HSBP}A_{HSBP}} + \left[\frac{1}{(h\cdot A_{fin}N_{fin}\eta_{fin})^{-1}} + \frac{1}{(h[A_t - N_{fin}A_{fin}])^{-1}}\right]^{-1} \tag{11}$$

In Equation 11, the acronyms HSBP, BP and TEG correspond to the values of the parameters specific to the heat sink base plate, aluminum base plate underneath the TEGs, and thermoelectric generators, respectively. N_{fin} is the number of fins on the heat sink; 29 in the final design. Fin parameters are shown in the following table, Table 6-1.

Table 6-1 Heat Sink Parameters

Name	Abbr.	Value	
Number of Fins	N_f	29	
Surface Area of a fin	A_f	0.002924	m^2
Total Heat Sink Area	A_t	0.086821	m^2
Single Fin Efficiency	η_f	0.9979	

By substituting this now known value for q back into each part's thermal resistance equation, the temperature drop across that part can be found. Summing the temperature drops allows the temperature at any point over the assembly to be found. The temperature drop that controls the voltage generation is measured by taking the difference between the temperatures calculated at points B and C in Figure 6-1.

To reduce unknowns and simplify the modeling process a number of assumptions were made. Aside from the assumptions associated with using the thermal resistance process itself, the largest deviation from reality was the exclusion of contact resistance between parts of the assembly. While this issue caused many problems during live testing, the final assembly will be tightly fit with thermal grease added to all interfaces. The grease should reduce the contact resistance to a point where the assumption causes minimal error in the model.

The final assembly utilizes a heat sink that is larger than the aluminum housing for the

generators. This means that the base of the heat sink overhangs the housing on all sides. To account for this, a conduction term for air from the heat source directly to the heat sink was added. The term uses a conduction coefficient for air calculated from a polynomial data fit to points given by Incropera et al. This polynomial is included as Equation 12. T_f in the equation is the film temperature, the average between the conducting surface and ambient temperature.

$$k_{air} = \left[(0.0045)T_f + (0.001)T_f^2\right] \cdot 10^{-3} \qquad (12)$$

Output from the Matlab simulation is plotted below. Figure 6-2 shows the expected temperature difference over the TEG, dT, plotted against various heat source temperatures and for various convection coefficients, h. Figure 6-3 shows the calculated voltage generation per TEG plotted against the same parameters.

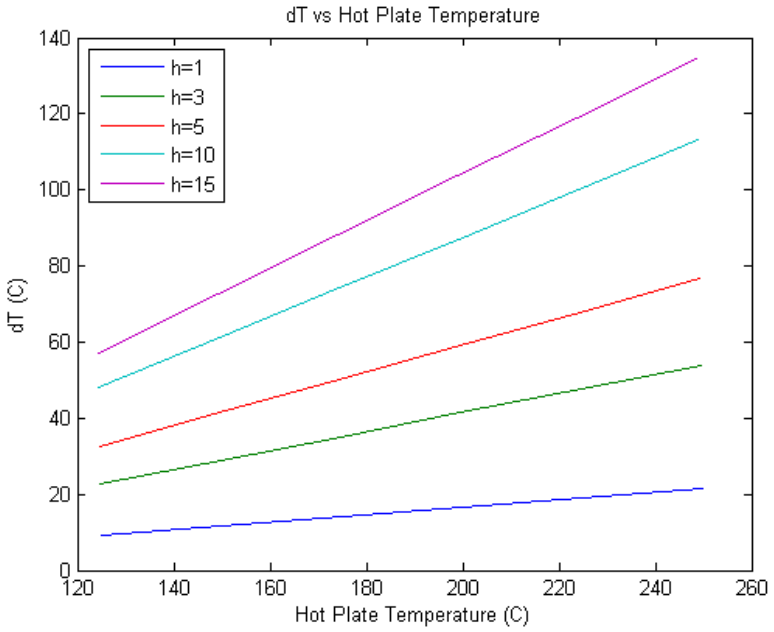

Figure 6-2 Matlab Model: dT against Source Temp

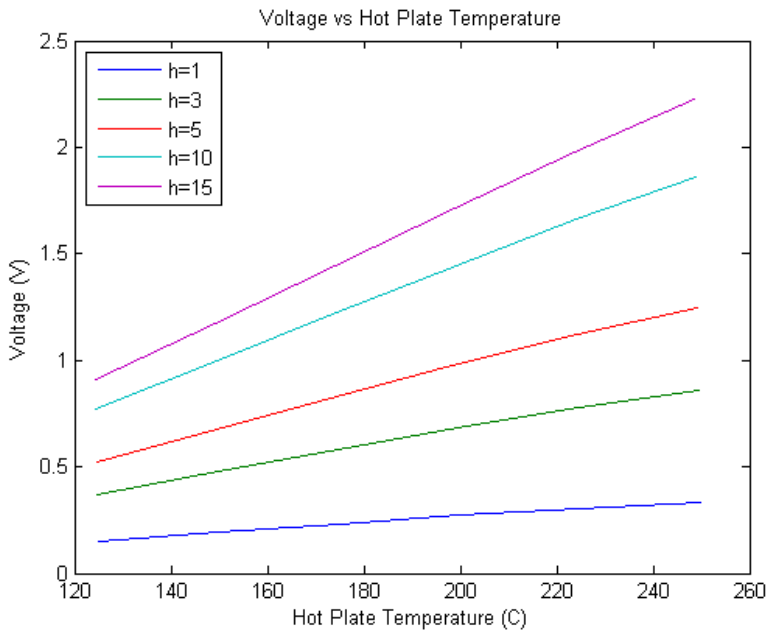

Figure 6-3 Matlab Model: Voltage against Source Temp

As can be seen, the driving factor behind increased voltage generation is the convection coefficient value, h. As h is increased, both the temperature difference achieved across the TEG and the voltage generated increase, as does the impact of the hot plate temperature. Once tests were run, correlations were made to determine the h value of the device. This allowed for the determination of unknown temperatures during the later tests. These results are presented in Section 8.

The code for the Matlab simulation can be found in Appendix B, Assembly Temperature Calculation and Assembly Voltage Calculation.

6.2 SolidWorks

To support the results from the thermal modeling performed in Matlab, both Solidworks and Ansys were used to create thermal models of the generator using the Solidworks Solid model of the design. These models were compared to the results of the Matlab simulations in order to give more confidence to the accuracy of the Matlab model. The calculated temperatures could then be used to determine an expected voltage generation given the specifications of Hi-Z's thermoelectric generators.

Using Solidworks and Ansys, each component of the device was assigned the materials used in the prototype. The material database in Solidworks and Ansys had the thermal properties of some of the materials used. However, the coefficients of thermal conductivity for some materials were not in the database, such as the thermo electric generators themselves. Custom coefficients of thermal conductivity were inputted into the software to model these materials using the values given by Hi-Z for the thermo electric generators. The material database from the Granta CES Edupack software (Granta Design Limited, 2009) was used to determine the thermal conductivity of the other materials, shown in Table 6-2. Boundary conditions were set to the values expected in the testing, and the simulations were run. Several tests were run with varying convection heat transfer coefficients for the heat sink as the exact coefficient was not known.

Table 6-2 Thermal Conductivities of Elements in Assembly

Material	Thermal Conductivity [W/m^2]
Aluminum	237
Thermoelectric generator	2.4
Silicone Gasket	0.6
Aluminum Heat Sink	237

There are several assumptions incorporated into these models. These assumptions are the source of discrepancies between the simulated and experimental results. There is assumed to be no contact resistance between neighboring surfaces, including the assumption that the bottom of the base plate is at the exact temperature of the heated surface. Conduction and radiation through the air gaps present in the device are also ignored in these simulations.

The results of the Matlab and Solidworks simulations differed due to differences in assumptions made between the models. The Matlab simulation modeled heat transfer through the air gaps present within the device, as well as heat transfer through the air gap between the heat source and the heat sink directly. The Ansys model omitted these.

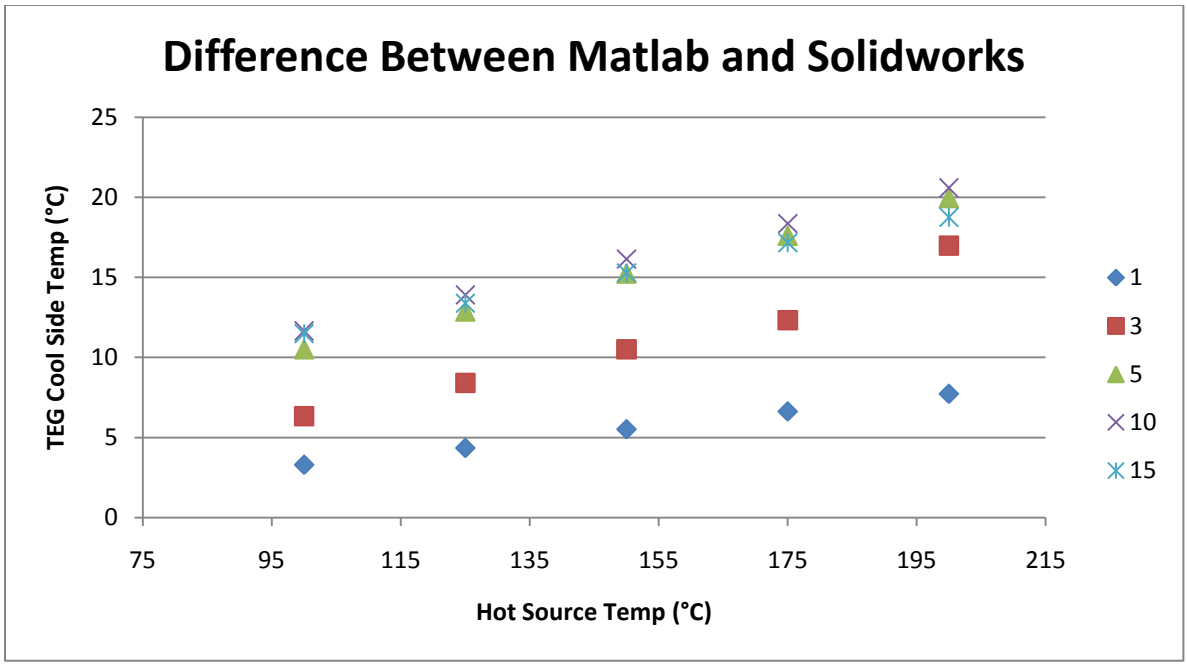

Figure 6-4 Difference in TEG Coolside Temperature

Figure 6-4 plots the temperature differences between the Matlab and Ansys simulations at multiple heat source temperatures and convection coefficient values. For each simulation run at a given heat source temperature with a given convection coefficient, the Matlab simulation gave higher temperatures at heat sink tip and the cool side of thermoelectric generator. It is assumed that the reason for this is the extra path modeled in Matlab between the heat source and the heat sink base directly allows more heat transfer to the heat sink. As all the parameters such as coefficients of thermal conductivity and device dimensions are consistent between the two simulations, it is believed that the results differ between the two because of the additional paths modeled in Matlab for the heat to pass through. Also, the method Ansys uses for calculating the heat transfer is unknown, so differences between the Ansys solution method and the thermal circuit method used in the Matlab simulation may also have led to the differing results.

7 Experimental Methodology

7.1 Thermal Tests

A testing program was used in order to validate the original designs and their performance. A further goal was to experimentally verify the theoretical results, thus providing an experimental corroboration between theory and practice in the design. Performance characteristics and limitations at different operating conditions were also identified and documented.

In order to fully design the system, including the location of various temperature sensitive components, the limitations of each component of the system were explored. Through a systematic approach, the effect of elevated temperature on each component was investigated. This allowed for the protection of temperature sensitive components. A detailed component failure test plan can be found in Appendix A, Part a) Test for Failure Mode.

Careful consideration was taken to ensure that sufficient data was collected that an accurate representation of what is actually occurring within the system could be established. Two thermocouples were used to monitor the system. The first was located on the hot surface in contact with the assembly and the second was attached to the tip of the heat sink. The remainder of the system can be defined using the simulation results. These temperatures were used together with the simulation results to estimate temperatures elsewhere on the assembly. The value of h, the convection coefficient, was calculated through experiments which, in

conjunction with the MatLab simulation, was used to estimate the cool side temperature of the generator.

A short term test was conducted to verify the correlation of temperature gradient and voltage. Once completed, a long term test was run to ensure the stability of the system over time and verify the endurance characteristics of the device. These test plans can be found in Appendix A, Part vb), Short and Long Term Testing.

7.2 Vibration Test

During operation, jet engines tend to vibrate with frequencies that are correlated to blade rpm in the turbines (Kerrebrock pp. 391-392). For a turbine rotating at 8000 rpm a single off balance blade would pass a stationary point 133 times per second, i.e. at a frequency of 133 Hz. The frequency of blade passing, for blade rows of 35 blades, is therefore approximately 4.5 kHz.

Kerrebrock notes an investigation into "buzz-saw" noise generation in engines. The study shows that in frequencies up to the blade passing frequency of 4.5 kHz there are numerous harmonics that cause resonance. Figure 7-1 below, reproduced from Kerrebrock, shows that at a critical frequency of approximately 1.55 kHz the maximum sound pressure level inside the engine under investigation is reached. Because Pratt and Whitney's specific engine performance characteristics are proprietary, the frequencies presented in Kerrebrock's data were used as benchmarks.

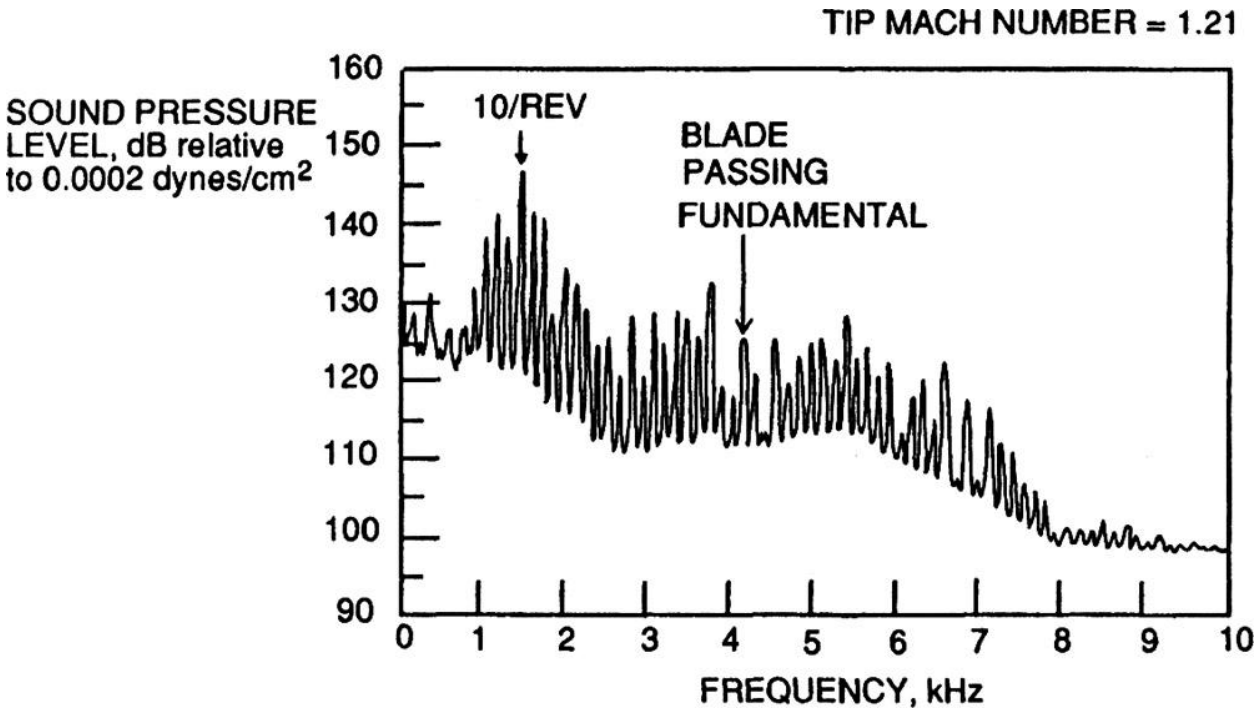

Figure 7-1 Sound Level against Blade Frequency (Kerrebrock p. 392)

The thermoelectric generator was vibration tested at 130 Hz, 1.55 kHz and 4.5 kHz. The goal of this test was to locate failure modes. Normally when conducting vibration tests, the goal is to determine resonance frequencies and operating modes of different devices (Smith, 1989). However, because the design is so far altered from the target design of four TEGs and a base plate sitting completely flush with the heat sink, this approach would not be useful. Testing at the three identified frequencies allowed the completion of low, medium and high frequency tests quickly and with a far reduced set of tools.

To test for vibration failure modes, the assembly was attached to a shaker at WPI. Using the shaker, tests were completed on the device at and around the three frequencies listed above at amplitudes on the order of 1/1000 of an inch. Before and after each test a visual inspection of the device was performed to check for faults such as loosening of the assembly's

adhesives or screws. Aliveness tests were also performed to ensure that non-visual faults had not occurred.

7.3 Challenges

Several problems were encountered during the initial testing of the device. Large discrepancies existed between the expected voltages and the voltages achieved, where the expected voltages were as much as two to three times as high as the voltages being measured. Solving this problem was a multiple step process involving many repeated tests.

One of the problems discovered was that the thermocouples prevented a flush connection between the TEGs and the heat sink. This reduced the amount of heat being drawn away from the cool side of the TEGs by the heat sink, leading to a lower temperature differential across the TEG. To solve this problem, the decision was made to mill gaps for the thermocouples in the base of the heat sink as well as the aluminum base plates. This solution allowed the heat sink to sit flush on top of the thermocouples and draw heat more effectively. Thermal paste was added to fill in the air pockets in the milled grooves which also served to increase the heat transfer.

Another problem found through testing was an electrical short between the leads of the TEGs and the aluminum heat sink. High temperature, electrically insulating tape was purchased to wrap around the leads and butt splices to prevent this. While an effective temporary solution, after repeated assemblies and disassemblies of the device the tape tended to wear and the short reappeared.

The most frustrating problem was the fragility of the leads of the HZ-2 modules. The leads are bundles of very fine wires and after being handled even a marginal amount would separate from the module. The first pair of generators was rendered completely useless in this manner with no warning. The chosen solution was to strengthen the connection between the

leads and the circuitry through the use of metallic butt splices. This meant that the leads, while still fragile, did not need to be manipulated as much during repeated tests. Hi-Z was contacted about the issue and responded that modules with solid leads are available per request. This style of module should be used in any future work as this type of failure is catastrophic to the device.

The butt splices were too large to fit into the old base plate and, as such, U shaped grooves were milled into the sides of the base plate. This gave the butt splices room to extend perpendicularly from the side of the base plate.

8 Results

8.1 Short Term Thermal Test

Prior to the steam pipe endurance test, a 5 hour performance test was run to ensure that the device was performing adequately. Figure 8-1 shows the data collected during this test. This included hot plate temperature (Heat Source Temp), heat sink fin tip temperature and device output voltage.

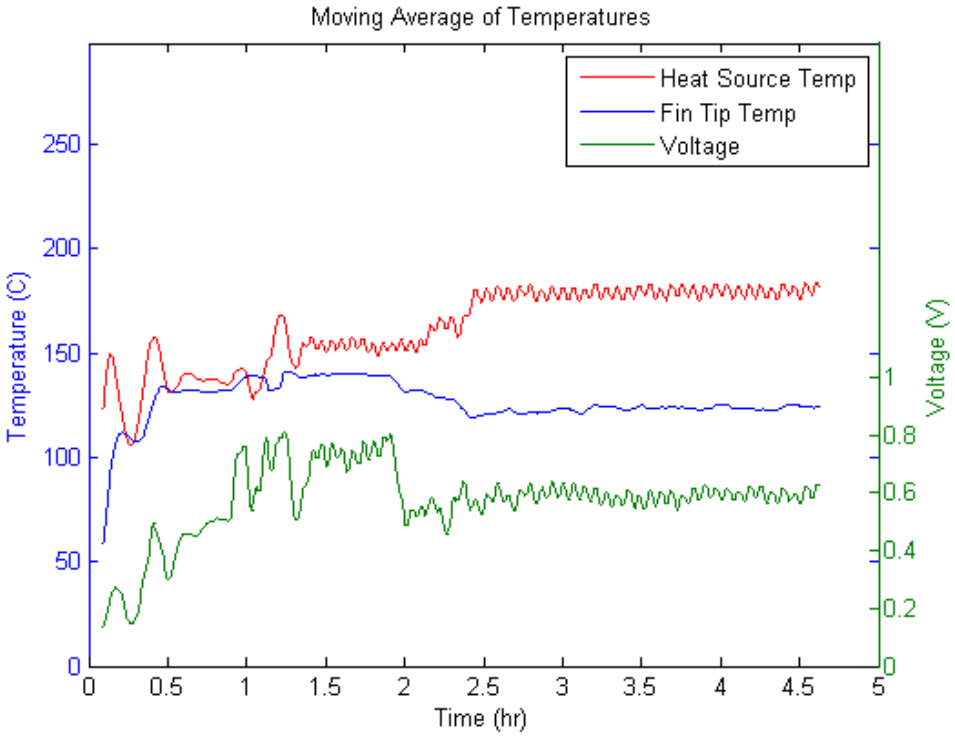

Figure 8-1 Short Term Data

The hot plate used during the test oscillated in order to maintain an average temperature. This oscillation caused a violent transient period in the beginning of the test as the heat sink attempted to establish equilibrium. This transient is evident in the data shown in

Figure 8-1 between up to 1.5 hrs. After the 2 hour mark, however, the data became relatively smooth as can be seen by the horizontal lines shown in Figure 8-1 for fin temperature and voltage generation.

During this period, the TEGs produced roughly 0.3V each. Because there was not a thermocouple directly in contact with the generators, the temperature differentials were backed out using the Matlab simulation and the Excel sheet provided by Hi-Z. Figure 8-2 shows 5 randomly selected sample points taken during the test plotted on the Matlab simulation results for voltage vs. hot plate temperature shown in Figure 6-2.

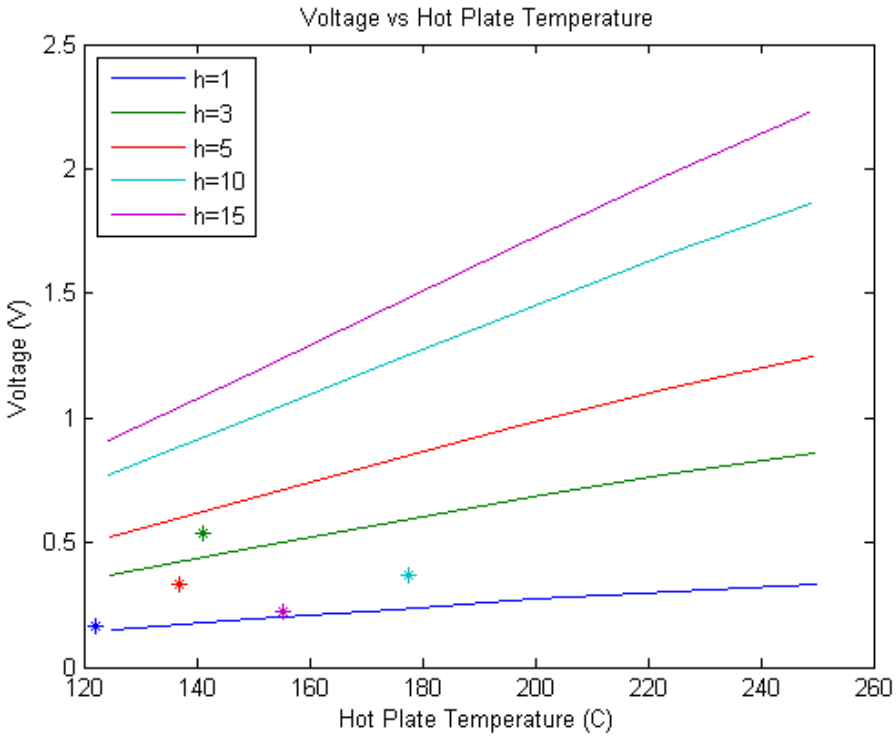

Figure 8-2 Matlab Comparison to Short Term Test

The experimental data points shown in Figure 8-2 correspond to an h value of approximately 2.5 W/m^2-K. According to the Matlab simulation, this corresponds to an approximate temperature difference of 30 °C. According to the Hi-Z spreadsheet, a 150 °C to 120 °C temperature drop produces 0.49 V per TEG. This is consistent with the results measured.

This test provided proof that the device is stable when exposed to steady state conditions. Despite the oscillations in the heat source, the device produced a steady voltage and did not overheat. The voltages produced, while lower than expected from the simulation results, were representative of the device's efficiency.

8.2 Long Term Thermal Test

A five day thermal test was run on a redundant steam pipe in the WPI Power House. The thermal stability of the pipe allowed steady state to be reached almost instantly by the generator. Due to an effective attachment solution not being found during this iteration of the project, the device was taped to the pipe using high temperature tape. The data acquisition system (DAQ) and breadboard circuit were taped to a nearby insulated pipe. Figure 8-3 shows the device from a top view attached to the steam pipe. Figure 8-4 shows the breadboard and DAQ taped to the insulated pipe. Finally, Figure 8-5 shows the complete setup including the data logging computer.

Figure 8-3 Long Term Test Setup Top

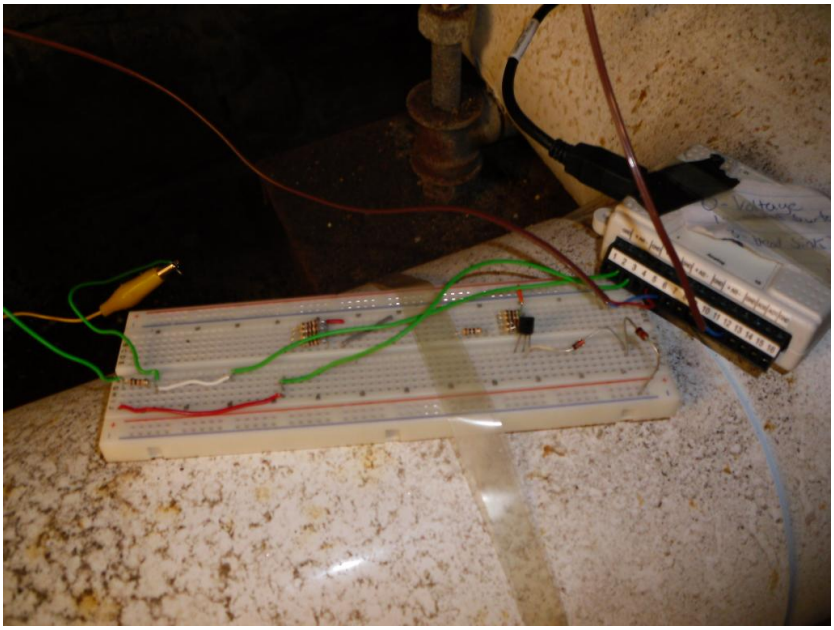

Figure 8-4 Long Term Test Breadboard and DAQ

Figure 8-5 Long Term Test Setup

Figure 8-6 shows the results of the test. The steam pipe temperature, the heat sink tip temperature and the voltage generation over a 1 kΩ resistor are shown. The voltages

generated by the device throughout the test were overwhelmingly low. The average generation was between 0.13 and 0.15 V. The average temperature of the steam pipe was between 140 and 150 °C, well under the maximum and optimum performance temperature of the HZ-2 generators. This does not explain the extremely low voltages, however.

Using the Matlab thermal model and adjusting for an ambient temperature of around 30 °C instead of the normal 25 °C, the voltage generation can be expected to be closer to 0.52 V. While this prediction is expected to be high, as it does not take many non-idealities into account, it reveals a substantial discrepancy between what was expected and what was generated.

There are a number of possible causes for the loss of voltage, but the overwhelming consensus is that the electrically insulating tape wore away through repeated assembly and disassembly of the device. This problem had occurred before and been fixed through reapplication of tape. The device was tested for shorts prior to the long term thermal test, but a short circuit is the only known failure that could cause such a dramatic loss of efficiency.

During one of the checks on the device, it was noticed that a thermocouple attached to the heat sink was not in contact with the metal. Rather, it was recording ambient temperature close to the heat sink. This was fixed by reattaching the probe to a more suitable location and subsequently the heat sink temperature took on a more appreciable value. This did not affect the fact that the voltage generation was still extremely low for the temperature regime.

A number of spikes appear on Figure 8-6. These data points are simply bad data.

Despite the low values of voltage generation, the test was successful in demonstrating the capability of the device for operating for over 115 hours continuously. After the first five hours of operation, the device was left to run with no supervision except the three times daily check to restart data collection. This experiment helped achieve the long term testing requirement set out by Pratt and Whitney.

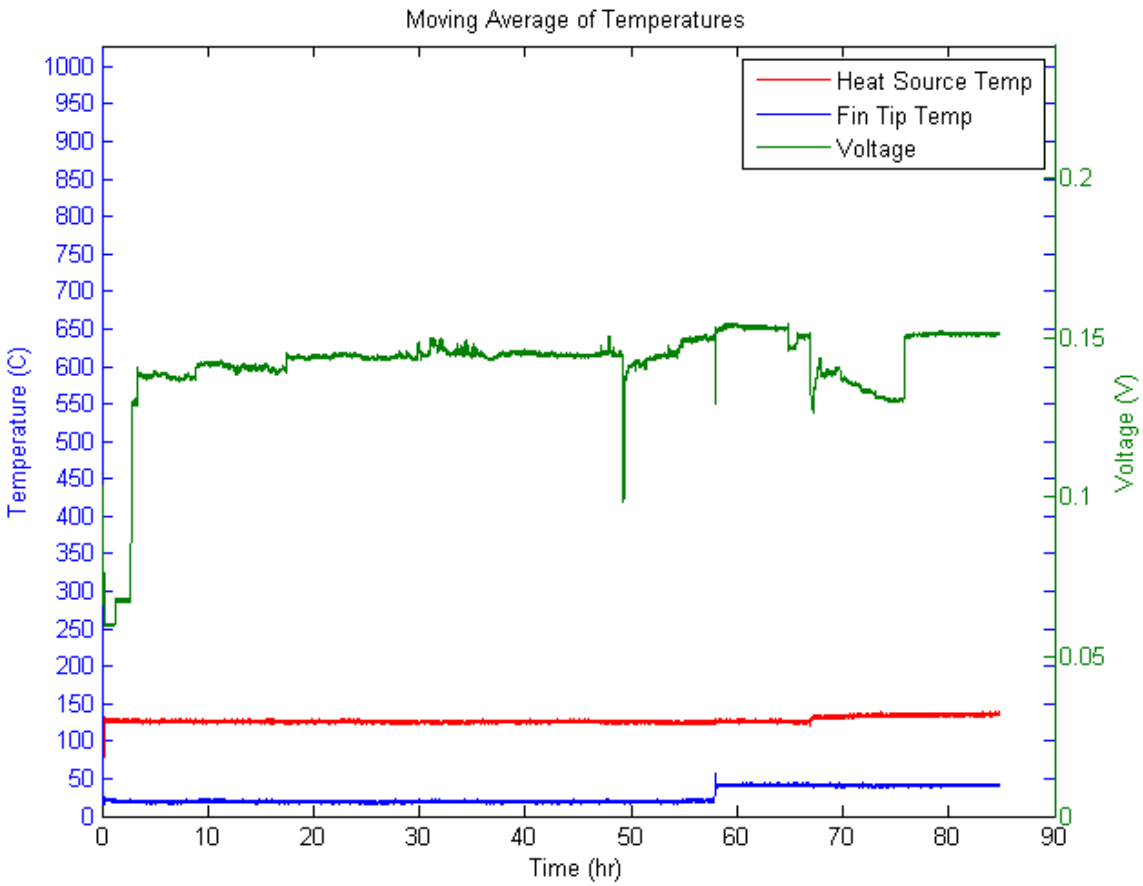

Figure 8-6 Endurance Test Data Plot

8.3 Vibration

The vibration test was successfully carried out on the assembly. Because of the circuit problems associated with the IC, the circuit itself was not included in the test. The device was tested at each of the three target frequencies, 140 Hz, 1.5 kHz and 4.5 kHz for 2 minutes each. Tests were also performed at ± 5% of the tested frequency to increase the spectrum of results.

At the low test frequency of 140 Hz, the assembly underwent 3.7 Gs of acceleration. This acceleration value increased to 4 Gs at the 1.5 kHz test frequency and finally reached 7 Gs at the highest test frequency of 4.5 kHz. These accelerations represented very high values of a stabilized engine on a test stand (Hall, 2010) and, as such, served to represent what the device could see under worst condition testing.

The device did not fail throughout the test. The leads of the TEGs were not damaged to any recordable degree and the assembly screws were still tight. Aliveness tests performed post test confirmed the device's fidelity. These positive results validated the design as stable and viable for future work.

9 Conclusion

A thermoelectric energy scavenging device was successfully constructed. The device is capable of transferring thermal energy into useable electric power. It can be left on a heat source indefinitely and continuously produce power. The assembly is very stable, easily passing vibration and thermal tests. The largest concern is short circuiting that drastically reduced performance of the device. With proper circuit design and a grounded heat sink, this can be made into a non-issue.

The device constructed, however, does not meet the requirements set forth by Pratt and Whitney. Voltage generation was more than an order of magnitude under the called-for amount, and power generation was far under the desired value as well. This is due to many factors. The efficiency of thermoelectric generators leaves much to be desired, with the modules used in this test a paltry 4.5% (Hi-Z). The cooling required to achieve the necessary temperature differential is most likely beyond the capability of passive cooling, but the addition of active cooling has many drawbacks itself. Finally, the use of metallic screws to hold the base plate to the heat sink provided a source of thermal leakage.

The ultimate goal of this design was to utilize four HZ-2 devices, each capable of producing 2.5V at a 150 °C temperature difference. This ideal situation would produce the 10V required by Pratt and Whitney. While this temperature differential is high, the work presented here suggests that the potential does exist for this device to be created and utilized with more advanced cooling technology.

10 Future Work

It is clear from the testing results that much work still needs to be done to meet the requirements set forward by Pratt and Whitney. Bradway et al started the project with proof of concept tests and an initial performance examination. The current tests were focused on determining how to increase efficiency and package the final device. Future work needs to be done to refine the current work and maximize the efficiency to the point where the device is effective enough to enter use on an engine test stand. Recommendations on how to accomplish this follow.

The generators used in the current iteration were very expensive. Because of budget constraints, it was impossible to buy the four required to even theoretically approach the design requirements. A device with the target number of generators should be built.

Cooling is a major concern of this device's efficiency. Keeping the temperature differential maximized for the life of the test is a challenge. Passive cooling should be the main topic of research as this method does not leech generated power. If a compromise between leeched and generated power can be found, such as in a high efficiency CPU or GPU fan, a smart circuit should be designed to utilize cooling to its maximum advantage. Other options include emerging technology such as unidirectional polymer heat sinks recently developed by a team at MIT (Dillow, 2010).

The method of mounting the device to various surfaces also needs to be refined. The tape used in experiments, while effective in an experiment, is not a design solution. Thermally conductive, electrically insulating adhesives would be a suitable starting point. The main

limiting factor, however, as has been the case with many of the components already part of the assembly, is the temperature range necessary for the final product. Many adhesive pads that are designed for high temperature applications do not have the thermal conductivity required to adequately transfer heat to the aluminum base plates. One thermally conductive pad offered by 3M only has a thermal conductivity value k = 0.6 W/m-K, almost 400 times lower than aluminum (3M, 2008).

Future work should miniaturize the current circuit and design and print custom circuit boards. Current work shows that a mounting point on a heat sink with an insulated enclosure and insulating tape is adequate, but more permanent mounting methods could be a topic of investigation.

Once the device is built, a complete set of testing should be undertaken. Performance curves at a wide range of temperatures should be constructed, documenting the output against various loads. A full spectrum vibration test will also need to be completed to ensure the internal circuitry will not be negatively affected by normal jet engine vibration.

11 Bibliography

Defense Industry Daily. [Online] http://www.defenseindustrydaily.com/images/ENG_F119_Thrust_Vectoring_Test_lg.jpg.

3M. 2008. *3M Thermally Conductive Adhesive Transfer Tapes.* St Paul, MN, United States : s.n., April 2008.

Bradway, Dustin, et al. 2008. *Thermal Energy Scavenging to Power Aircraft Test Sensors.* Worcester : Worcester Polytechnic Institute, 2008.

Dillow, Clay. 2010. New Plastic Conducts Heat Better Than Metals, But Only in One Direction. *Popular Science.* [Online] March 9, 2010. [Cited: March 25, 2010.] http://www.popsci.com/science/article/2010-03/new-polymer-conducts-better-metals-only-one-direction.

Encyclopedia Britannica. 2010. Encyclopedia Britannica. *Encyclopedia Britannica Online.* [Online] 2010. [Cited: March 12, 2919.] http://www.britannica.com/EBchecked/topic/591615/thermoelectric-power-generator.

Granta Design Limited. 2009. *CES EduPack.* Cambridge, UK : s.n., 2009.

Hall, John. 2010. *Vibration Testing.* [interv.] Joseph Miller. March 22, 2010.

Hi-Z. Hi-Z Technologies, Inc. *Hi-Z Technologies.* [Online] http://www.hi-z.com.

Incropera, Frank P, et al. 2006. *Introduction to Heat Transfer 5th Edition.* s.l. : Wiley, 2006.

Kerrebrock, Jack L. 1992. *Aircraft Engines and Gas Turbines 2nd Ed.* Cambridge : MIT Press, 1992.

SANYO. Material Safety Data Sheets - MSDS - Batteries Plus. *Batteries Plus.* [Online] [Cited: March 25, 2010.] http://www.batteriesplus.com/msds/Sanyo%20NiMH%206-03.pdf.

Smith, J D. 1989. *Vibration Measurement and Analysis.* London : Butterworths, 1989.

TEG Power. 2009. TEG Power. *TEGPower.com.* [Online] 2009. http://tegpower.com/index.html.

Teraoka, Hirohito. Development of Low Self-discharge Nickel-Metal Hydride Battery. *Eneloop.* [Online] [Cited: March 23, 2010.] http://www.eneloop.info/fileadmin/EDITORS/ENELOOP/ARTICLES/Teraoka_Article_EN.pdf.

Appendices

A. Test Plans

a. Test for Failure Mode

Objective: Determine the modes and points of failure of each component of the energy harvesting system.

Components to be tested:

1. Thermo Electric Generator
2. Aluminum plates
3. Wiring
4. Heat sink
5. Fan
6. NiMH battery
7. Electric Circuitry

Procedure:

Thermo Electric Generator

1. Turn on hot plate to 160 C.
2. Place TEG on hot plate.
3. Measure output voltage and temperature of TEG
4. Increase the temperature in 10 °C increments until failure. (Note: The manufacturer specifies a maximum Temperature of 260 °C).

5. Record if voltage generation degrades at higher temperatures, and if unit fails.

Aluminum plates

1. Turn on hot plate to 400 C.
2. Place Al plate on hot plate.
3. Increase the temperature in 50 °C increments until failure. (The melting point of Al is 660 °C).
4. Watch for any signs of failure.

Wiring

1. Wrap hotplate surface in aluminum foil
2. Turn on hot plate to 80 °C.
3. Place wires on hotplate
4. Increase the temperature in 10 °C increments until failure. (Expected failure for wire insulation is between 100 °C and 300 °C).
5. Observe for insulation melting

NiMH

1. Wrap hotplate surface in aluminum foil
2. Ensure that the hotplate is behind a protective polycarbonate shielding.
3. Have fire extinguisher on hand.
4. Turn on hot plate to 40 °C
5. Place battery on hotplate.

6. Increase the temperature in 5 °C increments until failure.
7. Measure voltage and temperature. Watch for failures.

Electrical Circuitry

1. Wrap hotplate surface in aluminum foil
2. Turn on hot plate to 30 °C
3. Place circuitry on hotplate.
4. Continuously check for complete circuit
5. Increase the temperature in 5 °C increments until failure.
6. Watch for blown capacitors, melting solder and open circuits

Analysis: Record the failure point and failure mode of each component.

b. Short and Long Term Testing

Objective: Explore the long term endurance of the energy harvesting device. Determine hot and cool side steady state temperatures given the ambient air temperature and the heat source temperature. Verify the equations derived that model the system.

Instrumentation:

1. Thermocouple – Heat source
2. Thermocouple – Heat sink
3. Voltage – Dummy load

Procedure:

1. Place energy harvesting device on the heat source
2. Begin recording data. Monitor constantly. Visually inspect the device for any component or system level failures.
3. Let test run for 5 hours.
4. Check for any failures.
5. Analyze data for stability
6. For Long Term Endurance Test: repeat for 5 days, monitoring the system every 6 hours.

Analysis:

Inspect the graphs of total voltage generated, and voltage across the dummy load for stability. Review the temperature of each of the components and ensure that the maximum temperature (including factor of safety) was never exceeded.

B. Matlab Code

a. Material Selection Code

```
%% Material Selection
% Sept 21 2009
% Matlab 7.5.0

clear; clc; close all;

%% Definitions
% Given
d_cer = .000032; d_gen = .0032; d_boundaryAir = .006;
k_cer = 2; k_gen = 1.2; k_boundaryAir = .0261;
T_hot = 453; T_ambient = 296;
A = .0036;

% Design param
d_mat = .006; k_mat = (100:500);
T_coolSide = zeros(length(k_mat),1);

%% Equations
dT = T_hot - T_ambient;

for i=1:length(k_mat)

    Qtot = (1/(d_mat/k_mat(i) + d_cer/k_cer + d_gen/k_gen + d_cer/k_cer +...
        d_mat/k_mat(i) + d_boundaryAir/k_boundaryAir))*A*dT;

    temp = d_mat/k_mat(i) + d_cer/k_cer + d_gen/k_gen + d_cer/k_cer +...
        d_mat/k_mat(i);

    T_coolSide(i) = T_hot - (Qtot * temp) / A; clear temp;
end

%% Plot
```

```
plot(k_mat, T_coolSide);
xlabel('Thermal Conductivity (W/m/K)'); ylabel('Cool Side Temp (K)');
```

b. Assembly Temperature Calculation

```
%%  TempEst
%  March 22, 2010
%
%  Estimates the temperature profile of the TEG assembly for a given
%  heat source temperature Tsource in degrees C and convection
%  coefficient h in W/m^2-K.  The coefficient represents the average
%  heat transfer to ambient from the heat sink on top of the assembly.
%
%  Typical values for Tsource are from 150 - 250 where 250 is the max
%  operating temperature of the TEG and many components of the assembly.
%
%  h values should be experimentally determined, values of between 5 and
%  30 have produced comparable results to tests.
%
%  [Thot,Tcool,Tfb,Tft,Rtot]=TempEst[Tsource,h]
%  Thot => Hot side of the TEG in C
%  Tcool => Cool side of the TEG in C
%  Tfb => Temperature at convective fin base in C
%  Tft => Temperature at tip of convective fin of heatsink in C
%  Rtot => Effective thermal resistance of assembly in K/W

function [Thot,Tcool,Tfb,Tft,Rtot]=TempEst(Tsource,h)

%% Constants
Tinf = 298;      %Room temp ~ 25C
Tinf = 305;      %Room temp ~ 32C
k_Al = 237;      %Cond. coeff of Al in W/m-K
k_Zn=112;        %Zinc
k_Alumina=2.5;   %Alumina - Ceramic screw
USE_FREE_CONV = false;
%% Generator Parameters from HZ-2 documentation
% Design hot side T = 230C (503K)
% Design cool side T = 30C (303K)
% Design flux q" = 9.54W/cm^2 = 95400 W/m^2
w_gen=.029; l_gen=.029; A_gen=w_gen*l_gen;
```

```
t_gen=.00508; k_gen = 2.4;

%% Assembly screws
% d_sc = 0.0035052;   %0.138" diameter screw
% A_sc = pi*d_sc^2/4;
% k_sc = 0;
% t_sc = 2*t_gen;     %Simplification based on t_bp=t_gen
%% Baseplate (bp) Parameters
w_bp=2*.029; l_bp=.029;
% A_bp=w_bp*l_bp+2*A_sc;
A_bp=w_bp*l_bp;
t_bp=t_gen; k_bp = k_Al;

%% Heat Sink Base Plate (hsbp) Parameters
w_hsbp=0.0667;                      %2 5/8" in m
l_hsbp=0.0762;                      %3" in m
t_hsbp=0.0111;                      %7/16" in m
A_hsbp=w_hsbp*l_hsbp; k_hsbp=k_Al;

% ------------------------- OLD HEAT SINK -----------------------------%
% w_hsbp=2*w_gen; l_hsbp=.029; %l_hsbp=2*w_gen; A_hsbp=w_hsbp*l_hsbp;
% t_hsbp=2*t_gen; k_hsbp=k_Al;
% ------------------------- OLD HEAT SINK -----------------------------%



%% Heat Sink Fin Parameters
N=29;                           %number of fins
t_fin=0.0015875;                %1/16" in m
w_fin=0.0667;                   %2 5/8" in m
l_fin=0.0206375;                %13/16" in m

% ------------------------- OLD HEAT SINK -----------------------------%
% N = 15;  t_fin = 2*w_gen/N;%Assume fin spacing equals fin width
% w_fin = 2*w_gen;            %Fins run parallel to long face of assembly
% l_fin = .0381;              %1.5 inch fins
% ------------------------- OLD HEAT SINK -----------------------------%
```

```
lc_fin = l_fin+(t_fin/2);       %Corrected fin lengh for eff estimation
P = 2*w_fin+2*t_fin;            %perimeter of a fin
Ac = t_fin*w_fin;               %Area of contact b/w fin and hsbp
Af = P*l_fin + Ac;              %Surface area of one fin
At = A_hsbp + N*(Af-Ac);        %Total area of HS available for convection
k_fin=k_Al;

%% Design Parameters
%Tsource=523;     %250C in K
Tsource=Tsource+273;
%h=5;               %Conv coeff over heatsink in W/m^2-K

%% The Circuit (outdated)

%% Free Convection Calculation
A_free=A_hsbp-A_bp; %Free convection occurs where TEGs don't touch heatsink
h_free=FreeConvCoeff(Tsource,Tinf,(t_bp+t_gen));
% if h_free < 0 %Ra out of range
%     disp('Free convection ignored, Ra invalid for correlation')
%     USE_FREE_CONV = false;
% end

%% Calculation of efficiency
m=sqrt(h*P/(k_fin*Ac));
fin_eff=tanh(m*lc_fin)/(m*lc_fin);  %Eq 3.89 Intro to Heat Xfer
% a=t_sc/(k_sc*2*A_sc);
b=t_bp/(k_bp*A_bp)+t_gen/(k_gen*2*A_gen);

if USE_FREE_CONV,
    c=1/(h_free*A_free);
else
    Tf=(Tsource+Tinf)/2;
    k_air=(.0001*Tf^2+.0045*Tf+13.685)*10^(-3);
    c=(t_bp+t_gen)/(k_air*A_free);
end

d=t_hsbp/(k_hsbp*A_hsbp);
```

```
e=1/(N*fin_eff*h*Af);
f=1/(h*(At-N*Af));

% Rtot=d+1/(1/a+1/b+1/c)+1/(1/e+1/f);
Rtot=d+1/(1/b+1/c)+1/(1/e+1/f);

q=(Tsource-Tinf)/Rtot;

%% Temperature Calculation
Thot=Tsource-q*t_bp/(k_bp*A_bp);
Tcool=Thot-q*t_gen/(k_gen*A_bp);
Tfb=Tcool-q*t_hsbp/(k_hsbp*A_hsbp);
Tft=1/(cosh(m*l_fin)+h/(m*k_fin)*sinh(m*l_fin))*(Tfb-Tinf)+Tinf;

Thot=Thot-273;Tcool=Tcool-273;Tfb=Tfb-273;Tft=Tft-273;
```

c. Assembly Voltage Calculation

```
%% Volt Calc
% Feb 28, 2010
%   This function uses constants taken from the HZ-2 prediction chart
%   provided by Hi-Z corp to predict the voltage across ONE HZ-2 TEG
%   from given temperatures Thot and Tcool.  The temperatures represent
%   the temperature seen by the TEG on its hot and cool side, respectively.
%   The temperatures should be provided in degrees Celsius.
%
%
%   [V_oc, V_ml] = VoltCalc(T_hot,T_cool) returns the open circuit and
%   matched load voltages for an HZ-2 TEG at temperatures T_hot and T_cool

function [V_oc,V_ml]=VoltCalc(Thot,Tcool)

%% Generator parameters
n_legs = 196;
% N-type constants
C1n=3.4691; C2n=-0.014202; C3n=0.000023254; C4n=-0.000000013;
% P-Type constants
C1p=-1.818175; C2p=0.01113344; C3p=-0.00002035; C4p=1.1344e-8;

%% Calculation

Tave = (Thot+Tcool)/2+273;
dT = Thot-Tcool;

alfa_n=-442.76+C1n*Tave+C2n*Tave^2+C3n*Tave^3+C4n*Tave^4;
alfa_p=161+C1p*Tave+C2p*Tave^2+C3p*Tave^3+C4p*Tave^4;

% Open circuit voltage across n- and p- type semiconductors
Voc_n=alfa_n*dT/1000;
Voc_p=alfa_p*dT/1000;

V_oc=0.89*(n_legs/2)*(-Voc_n+Voc_p)/1000;
```

```
V_ml=V_oc/2;

% voltage=[V_oc,V_ml];
```